P11R.15 DROP AXIS RATIO AND FALL VELOCITY DISTRIBUTIONS FROM 2-D VIDEO DISDROMETER

Merhala Thurai[1], V.N. Bringi[1]*, K. Nakagawa[2], T. Kozu[3], M. Schoenhuber[4] and T. Shimomai[3]
[1]Colorado State University, Fort Collins, Colorado, USA
[2]National Institute for Information and Communications Technology, Japan
[3]Shimane University, Matsue, Japan
[4]Joanneum Research, Graz, Austria

1. INTRODUCTION

Drop axis ratios and terminal fall velocities in rain are important for several reasons. The former is particularly needed for weather radars employing dual-polarization technique, which estimate the rainfall rate from the co-polar and differential reflectivity which in turn requires accurate knowledge of the axis ratio dependence on the equivalent drop diameter (Goddard and Cherry 1984). This is even more important for weather radars operating at C-band and above, to correct for co-polar and differential attenuation of the radar beams traversing the rain-filled medium (Bringi et al 2005a). The fall velocities on the other hand are more needed for vertically-pointing rain radars, which try to estimate the drop size distribution from the Doppler velocity spectrum measured along the vertical (Kobayashi and Adachi, 2005). Moreover, studies relating to the modeling of the melting layer require the fall velocity to be accurately characterized in rain, soon after the completion of melting (Awaka et al et al 1985).

In an earlier study, it was shown that it was possible to obtain distributions of both parameters in terms of the equivalent drop diameter (Thurai and Bringi, 2005) using a two-dimensional video disdrometer (Randeu et al 2002). Under calm conditions, drops were generated from a hose located on a bridge 80 m above ground (Jauntal bridge in Carinthia, Austria), this height being sufficient to allow drop oscillations to reach steady state. The disdrometer data had to be carefully processed so as to eliminate the drops mismatched by the instrument and to remove the system spreading function. The total number of drops analyzed was around 115,000. Their axis ratio distributions were obtained for diameters ranging from 1.5 to 9 mm. The mean axis ratio decreases with increasing drop diameter, in agreement with the upper bound of the Beard and Chuang (1987) equilibrium shape model (BC87). The inferred mode of oscillation appeared to be dominated by the oblate-prolate axisymmetric mode for the diameter range 1.5 to 9 mm. The drop terminal velocities were also measured and these showed very good agreement with Gunn and Kinzer (1949) data as well as the Beard and Pruppacher (1969) data.

*Corresponding author address:
V. N. Bringi, Dept. of Electrical Engineering, Colorado State University, Fort Collins, CO 80523-1373, USA.
Email: bringi@engr.colostate.edu

In this paper, we report similar measurements made in natural rain in various locations. The results of the analyses are compared with the 80 m bridge results used as reference.

2. VIDEO DISDROMETER MEASUREMENTS

Two mid-latitude locations (Tokyo in Japan and Colorado, USA), one sub-tropical location (Okinawa, Japan) and two tropical locations (San Juan, Puerto Rico and Sumatra, Indonesia) are used for this comparative study. The measurements were made using different models of the same instrument. In the case of Okinawa, it was also possible to examine the regime dependence, by analyzing the data collected during (i) warm shallow rain, (ii) normal Baiu event and (iii) a prolonged, intense event during the Baiu season. The cases are summarized in Table 1.

Table 1: Location of 2D-VD measurements

Case	Location	comments
a	Tokyo (mid-latitude)	Data during summer/autumn
b	Colorado (mid-latitude altitude = 1.6 km)	Data during summer
c	Okinawa (sub-tropical, oceanic)	Events separated into (1) shallow rain (2) normal Baiu (3) intense Baiu
d	San Juan, PR (tropical)	Non-hurricane events only
e	Sumatra (tropical altitude = 0.85 km)	Plane test not yet performed for the 2D-VD

In most cases, only the measurements made during low wind conditions were used. This was to minimize the extraneous effects introduced by the artificial winds in and around the 2D-VD sensor area. The only exception was c(3) which is the subject of another study (see Bringi et al, 2005b, this issue). For the cases of b, c(3) and d, the measured drops were rematched in order to remove problems that arose with mismatched drops during heavy precipitation. Small drops particularly those with smaller diameters than 1.5 mm needed to be rematched.

3. AXIS RATIO DISTRIBUTIONS

One example of axis ratio distribution is given in Fig. 1, which shows the number of drops on a log scale in terms of the axis ratio and equivalent diameter. The data were taken during the 'Baiu' season in Okinawa, Japan, a sub-tropical, oceanic location during May and June of 2004. All data were used to derive this distribution, except for the 8th and the 9th of June which was an exceptionally intense event. These two days were examined separately because of the prolonged and intense nature of this event, and in fact is the subject of another paper (Bringi et al 2005b), and referred to later, which uses the 2D-VD measurements to examine the retrievals from an advanced C-band dual-polarization radar as well as a 400 MHz wind-profiler.

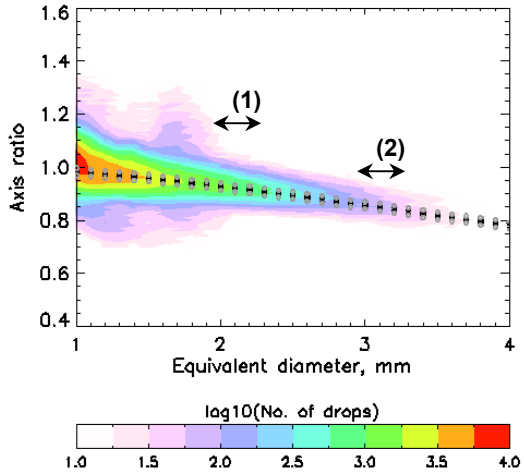

Fig. 1. Axis ratio versus equivalent diameter from the 2D-VD data taken during the Baiu season in 2004. The color scale of the intensity plot contours the number of drops within an axis ratio and a diameter interval on a $\log_{10}$ scale.

For the normal Baiu event shown in Fig. 1, the axis ratios followed a trend similar to that observed with the previously reported artificial rain experiment (Thurai and Bringi, 2005). The ratios lie in the upper bound of the BC87 model predictions. The curves corresponding to the BC87 mean ratios as well as their upper and lower bounds are also included in the figure.

Measured distributions for diameter intervals 2.0-2.5 mm and 3.0-3.5 mm, marked as (1) and (2) respectively in Fig 1, are shown in Fig. 2. Superimposed in red are the corresponding Gaussian fitted curves. These curves seem to represent the measurements fairly accurately, although a small amount of skewness is seen for the 3-3.5 mm case towards larger axis ratios.

In almost all cases, the axis ratio distributions could be fitted to Gaussian functions, although some skewness was observed for diameters larger than 3 mm. This was not only the case with the Okinawa Baiu data shown in Fig. 1 but also for almost all the 2D-VD data obtained in all other locations in Table 1. A summary of all the fitted parameters are shown in Table 2 and compared with the reference bridge data for various diameter intervals. For comparison, the mean axis ratios corresponding to BC87 equilibrium model are also given. In most cases, the measured axis ratios are somewhat higher than the equilibrium model. As with the bridge experiment data, the measured axis ratios in rain were in fact closer to the upper bound of the BC model. Note, those given in red in Table 2 had less than 100 drops in the category and hence their Gaussian fits may not be very accurate. This was particularly the case beyond 5 mm in natural rain.

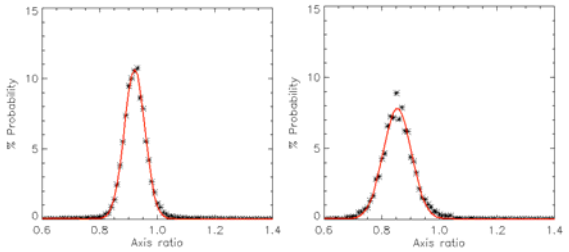

Fig. 2: Axis ratio distributions for diameter intervals 2.0-2.5 mm (left) and 3.0-3.5 mm (right). Superimposed in red are the Gaussian fitted curves

Fig. 3 shows the contour intensity plot for all the rain events given in Table 2, excluding Sumatra data which had a slight uncertainty in the calibration of the distance between the two light planes of the 2D-VD. Superimposed on the plot is the BC87 curve. They represent a total number of drops exceeding 10^6.

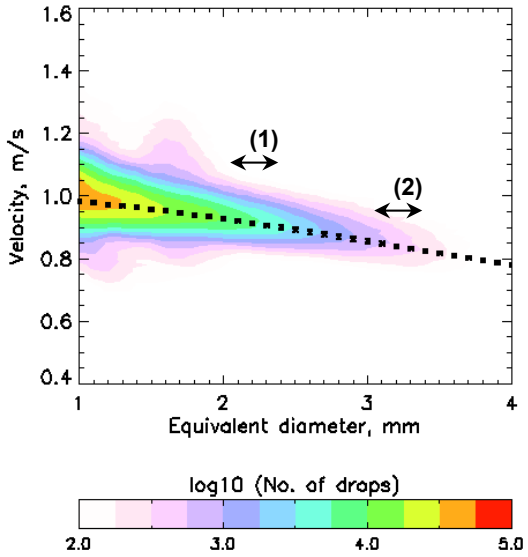

Fig. 3. Axis ratio versus equivalent diameter for all the 2D-VD data taken in rain. The color scale of the intensity plot contours the number of drops within an axis ratio and a diameter interval on a $\log_{10}$ scale. The BC curve is over-plotted for comparison

The axis ratio distributions for the whole rain data-set were determined as before. Once again, two examples are shown here. Fig. 4 shows the over all distributions in blue for the two diameter intervals 2.0-2.5 mm and 3.0-3.5 mm, marked as (1) and (2) respectively in Fig 3. These are compared with the previously reported distributions from the artificial rain from the 80 m fall bridge experiment. The larger diameter interval shows noticeable difference; whilst the artificial rain distribution could be fitted to Gaussian (also included in the figure), the natural rain data show finite skewness. This was also the case for 4.0-4.5 mm and 4.5-5.0 mm diameter intervals (not shown here). For smaller diameters, as in the case of 2.0-2.5 mm (left plot of Fig. 4), no significant differences were seen between the artificial rain and the natural rain data. (Both could be fitted to almost the same Gaussian curves). As a general observation, the differences between the two sets of data became noticeable for diameter intervals beyond 3 mm, with the natural rain data showing slight skewness.

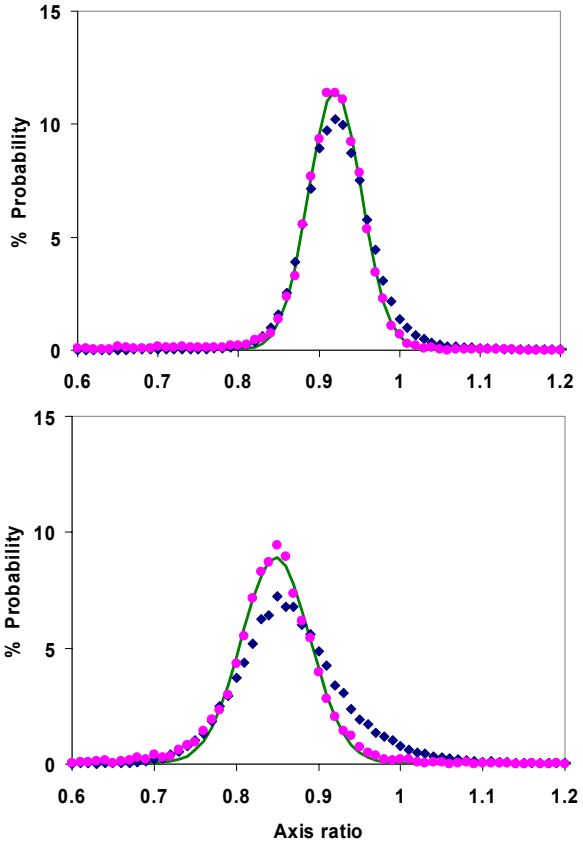

Fig. 4: Axis ratio distributions (blue diamonds) for diameter intervals 2.0-2.5 mm (left) and 3.0-3.5 mm (right) for the overall distributions derived for rain, compared with the corresponding distributions for the artificial rain from the bridge experiment (magenta dots) and their fitted Gaussians (green lines).

Fig. 5 shows the mean and one half the standard deviations of the total data set (excluding the Sumatra data) for rain for various diameter intervals. The overall mean is also shown and compared with the mean of the axis ratio distributions derived from the bridge experiment with the artificial rain, shown as magenta dots. For completion, the BC87 curve is included as well as the laboratory measurements from Beard and Kubesh (1991) for small drops. The latter merges very well with both our artificial rain data and our natural rain data.

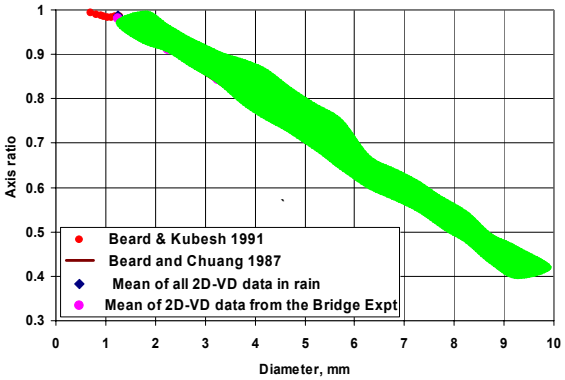

Fig. 5: Range of measured mean axis ratios in rain shown as green shaded area, represented by the overall mean (shown as blue diamonds) and one half of their standard deviations. Overlaid are the mean axis ratios from the artificial rain study (from the bridge experiment) and the laboratory measurements for small drops as well as the BC87 curve.

4. FALL VELOCITY MEASUREMENTS

In the earlier study which reported measurements from the artificial rain experiment (Thurai and Bringi 2005), it was found that the 2D-VD was also capable of accurately measuring the fall velocity of water drops. Drops with diameters up to 9 mm were analyzed. Their mean velocity results were in close agreement with Gunn-Kinzer (GK) data for diameters up to 5 mm after a small adjustment to take into account the height of the experiment location. More interestingly, the results showed excellent agreement with a previously published fourth order fit (Brandes et al 2002) based not just on GK data but also on Beard and Pruppacher (1969) data which ranges up to 8 mm drop diameter.

A similar attempt was made in this study using the data in rain from all the locations mentioned earlier. The results are summarized in Table 3 and compared with the fit to the GK data. In the case of Colorado, the mean velocities are seen to be significantly higher GK fit. However, when adjusting for the altitude of the 2D-VD location (with an adjustment factor of 1.06 for an altitude of 1500 m a.s.l., from Foote and du Toit, 1969), the mean velocities can be shown to be consistent with the GK fit. Similarly, adjustment factors of 1.035 for Sumatra and 1.018 for the 80 m bridge experiment also reduce the measured mean velocities

to agree well with the GK fit. Other locations are close to sea level and the close agreement to the GK data can be seen without any adjustment to the measured mean velocities.

Fig. 6 shows the color intensity plot for the velocity distribution in terms of the drop diameter for the normal Okinawa Baiu events. The distribution follows the GK curve which is superimposed on the plot. No adjustment factor is necessary since the location is only 90 m a.s.l.

As with the axis ratio analyses, the fall velocity distributions were also examined for individual diameter intervals. Two examples are shown in Fig. 7, the distributions being extracted from the Okinawa Baiu data in 2004 shown in Fig. 3. The two histograms correspond to 2.0±0.1 mm and 3.0±0.1 mm respectively. The superimposed red curves show the best Gaussian fits, which seem reasonable approximations.

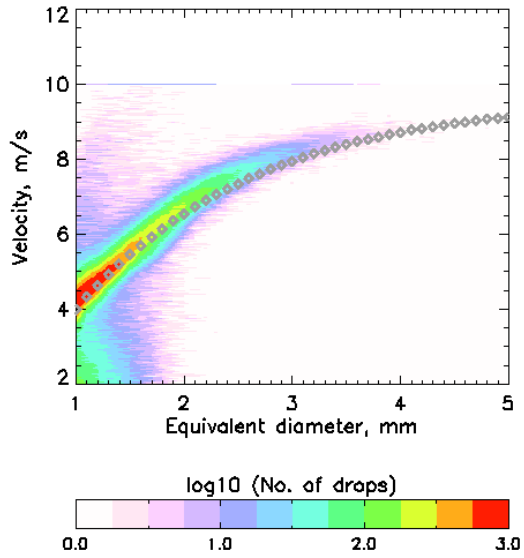

Fig. 6. Fall velocity versus equivalent diameter for the Baiu season in 2004. The color scale of the intensity plot contours the number of drops within velocity and diameter interval on a $\log_{10}$ scale.

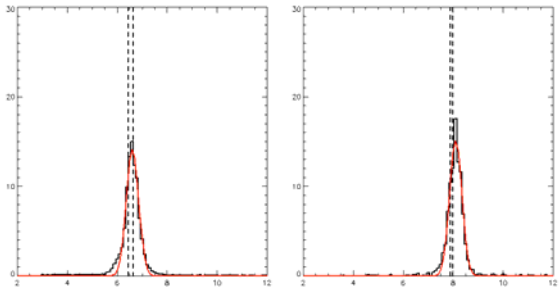

Fig. 7: Fall velocity distributions for diameter intervals 2.0±0.1 mm (left) and 3.0±0.1 mm (right). Superimposed in red are the Gaussian fitted curves. Dashed lines represent the expected interval from the GK data.

Once again, as was the case with the axis ratio distributions, all velocity histograms in all cases could be fitted to Gaussian functions. The mean and the standard deviations given in Table 3 do indeed represent these fitted values. The standard deviations are significantly higher than the expected GK range (for example as seen in Fig. 5), which presumably is due to the presence of vertical wind velocity and/or turbulence in and around the sensor area. This seems noticeable, despite the fact the only the low-wind cases were chosen for these analyses. It should also be noted that the Koganei case shows the largest spread, which could be due to the 2D-VD being located on the roof-top of a 4-floor building.

5. AN EXAMPLE APPLICATION

As mentioned in section 1, drop axis ratio dependence on equivalent drop diameter is an important parameter needed by retrieval algorithms for (linear) dual polarization weather radar. It is needed for not just deriving rainfall rates more accurately but also correcting for rain attenuation along the radar beam. In the accompanying paper (Bringi et al 2005b, this issue), one method for doing this at C-band was described. The radar uses the measured profiles of co-polar reflectivity (Z_h), differential reflectivity (Z_{dr}) and differential phase (Φ_{dp}) and the self consistency principle to correct for attenuation and successfully retrieve the drop size distribution (*dsd)*. Central to these calculations is the relationship between the specific co-polar attenuation (A_h), specific differential attenuation (A_{dp}) and the differential phase (K_{dp}) at C-band, given in in the accompanying paper (Bringi et a2005b) and repeated below.

$$A_h = 0.05623 K_{dp};\ \mathrm{dB/km} \qquad (1a)$$

$$A_{dp} = 0.00736 K_{dp}^{1.133};\ \mathrm{dB/km} \qquad (1b)$$

$$\frac{K_{dp}}{Z_h^{linear}} = 4 \bullet 10^{-5} \left(Z_{dr}^{0.447} \right);\ \mathrm{deg/km\,per\,mm^6\ m^{-3}} \qquad (2)$$

These were specific to the heavy/intense event that occurred during the Baiu season in 2004 in Okinawa. Figure 6 shows the mean axis ratio versus the equivalent diameter derived from the 2D-VD data for this event. These are the same values as those in Table 2 under column Ogimi (Okinawa) – Baiu – heavy. The best-fitted curve for these axis ratios is also shown in the plot, given by the cubic fit :

$$\frac{b}{a} = 1.077 - 0.0964 D + 0.0197 D^2 - 0.0032 D^3 \qquad (3)$$

$$for\ \ 1.75 \le D \le 3.75\,mm$$

Using this empirically fitted equation and using the 1-minute integrated *dsd* measured by the 2D-VD data for the prolonged Ogimi event, T-matrix calculations

were made to determine Z_h, Z_{dr}, K_{dp}, A_h and A_{dp} for each of the 1-minute dsds.

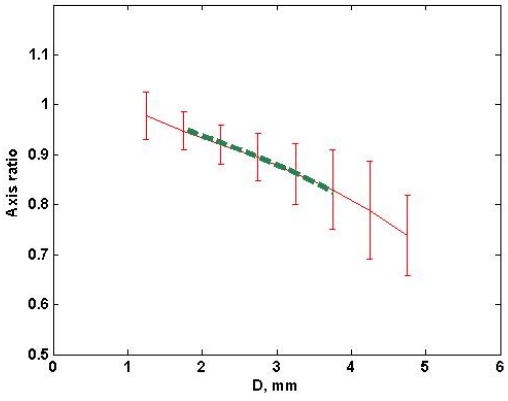

Fig. 8: Mean drop axis ratio and standard deviation as a function of drop diameter, derived for the prolonged and heavy/intense 2004 Baiu event in Okinawa. The green line shows the best-fitted line.

Fig. 7(a) shows the scatter-plot between A_h and K_{dp} derived from the 1 minute dsd, together with the straight line fit of equation (1a) given in red. Fig. 7(b) shows the corresponding scatter-plot between A_{dp} and K_{dp}, A_{dp} being plotted on a log scale to demonstrate that a power law relationship between A_{dp} and K_{dp} could be derived. The best fitted equation 2(b) is also included in Fig. 7(b) as the red line. One can apply the best-fit coefficients to correct for the co-polar and differential attenuation for the measured Z_h and Z_{dr}. One example is given in Fig. 10(a), (b) and (c) which are PPI scans of measured Z_h, measured Z_{dr} and measured Φ_{dp}.

Using the correction method given in the accompanying paper and the 2D-VD derived coefficients in equations 1(a), 1(b) and (2), it is possible to restore the true reflectivity and the differential reflectivity and use these to estimate the differential propagation phase. Fig. 11 compares the estimated Φ_{dp} and the measured Φ_{dp} for the PPI scan in Fig. 10. The best fit straight line shown in red has a gradient of 1.042. Good agreement is seen which gives credibility to the attenuation correction scheme adopted in the inter-comparison study. For more operational purposes, it would be more appropriate to examine the differences in the measured and estimated Φ_{dp} at the edges of the PPI scan (as oppose to the whole scan) as has been done in the accompanying paper (Bringi et al 2005b).

Finally, it is important to note that the fitted coefficients given in equations 1(a), 1(b) and 2, and the corresponding the red lines in Fig 9(a), 9(b) and 9(c), are unique to this particular event and should not be used as universal coefficients. Nevertheless, the usefulness of simultaneous 2D-VD measurements has been demonstrated in this important application. There are of course other applications of drop shapes and fall velocities, see for example, Steiner et al (1991).

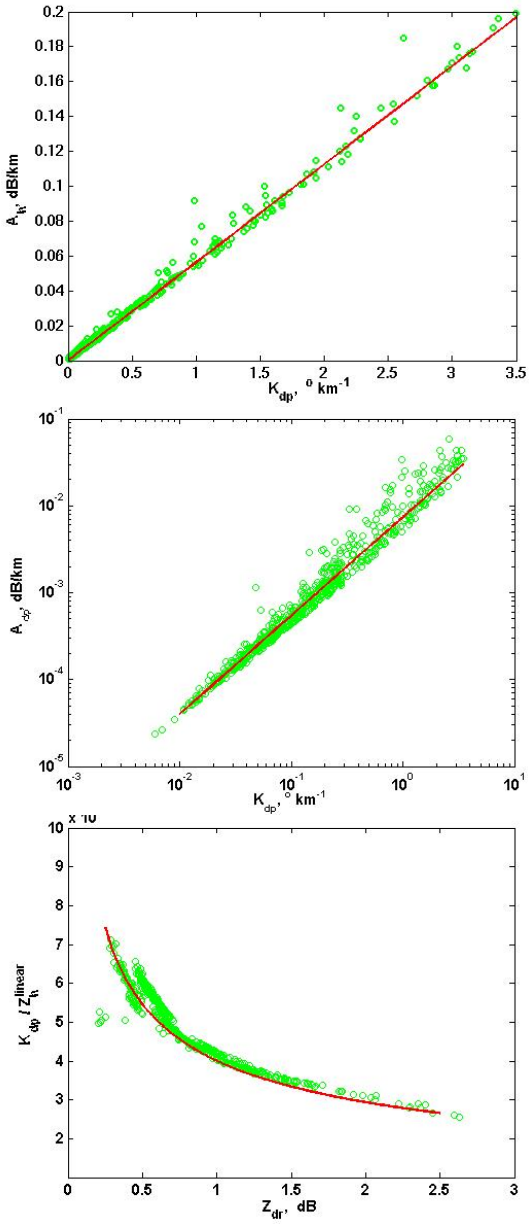

Fig. 9: Relationships between A_h and K_{dp} (top), Adp and K_{dp} (middle) and K_{dp} / Z_h^{linear} and Z_{dr} (bottom) derived from the 1 minute integrated dsds and the drop axis ratios derived from the 2D-VD for the Ogimi-Baiu 2004 heavy event. Superimposed in red are the best-fit curves which were used in the retrieval method for a C-band dual polarization radar located nearby (results in the accompanying paper, Bringi et al 2005b, this issue).

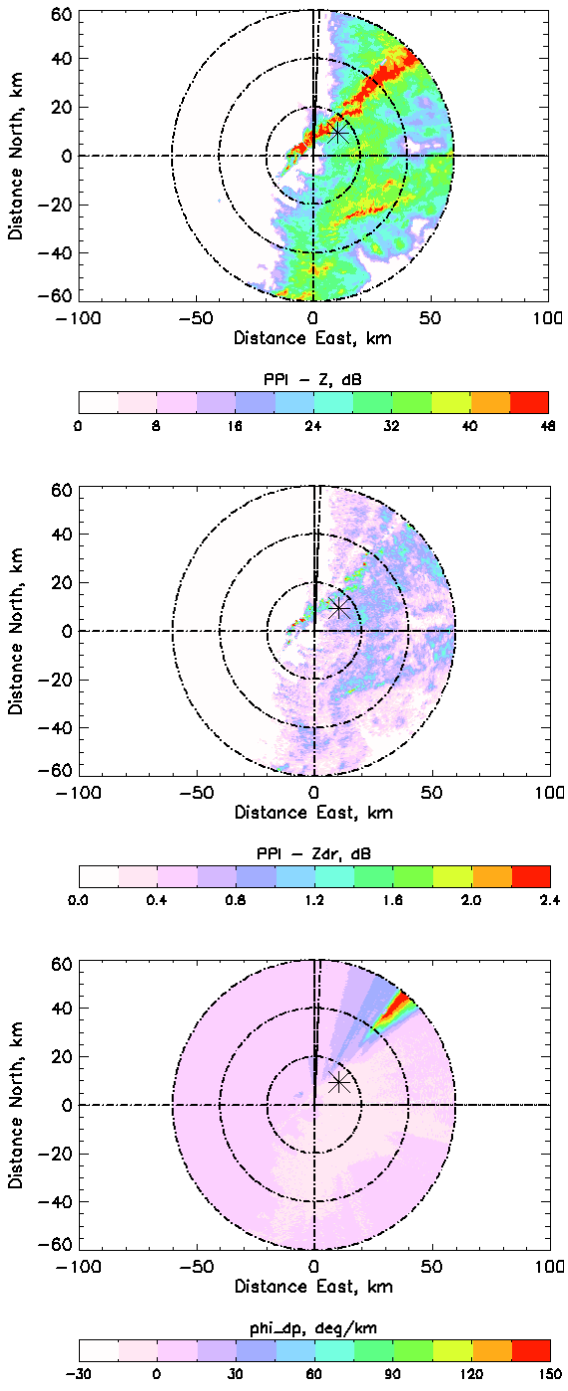

Fig 10: An example of the PPI scan during the 2004 intense Baiu event in Okinawa, for which the axis ratio dependent coefficients were derived using the 2D-VD data, given in equations 1(a), 1(b) and (2). Top plot shows the measured reflectivity, the middle panel shows the differential reflectivity and the bottom panel shows the differential phase

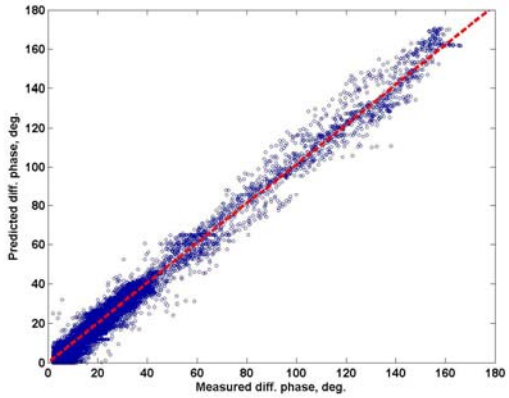

Fig 11: Estimated Φ_{dp} versus the measured Φ_{dp} for the PPI example of Fig. 10, after correcting for the C-band attenuation using the 2D-VD derived drop axis ratios and *dsd*'s. The red line is the best fit line, which has a gradient of 1.042.

5. CONCLUSION

Drop axis ratio and fall velocity measurements measured in rain have been analyzed from a number of locations. Analyses of the axis ratio distributions indicate that their variation with equivalent diameter may be location and/or rain regime dependent. When the overall distributions were compared with those obtained from a previous study using artificial rain data, slight skewness was observed for the larger diameter drops (above 3 mm). For smaller drops no significant differences were observed. The differences and the skewness were only evident in the 3 – 5 mm diameter range. However, the mean from the previous study lies within one half of the the standard deviation of the present results. The present results merge very well with some previously published laboratory data for small drops.

One example application of the axis ratio measurements from the 2D-VD was demonstrated for a C-band dual-polarisation radar retrieval algorithm. The 2D-VD data were used to derive the relationships between the radar measured parameters (Z_h, Z_{dr} and Φ_{dp}) which in turn were used to correct for attenuation The reconstructed Φ_{dp} using the corrected Z_h and Z_{dr} were in good agreement with the measured Φ_{dp}. This has several implications as demonstrated in the accompanying paper. However, it is important to note that the 2D-VD derived relationships were specific to the event studied.

Fall velocity measurements from the 2D-VD in rain showed good agreement with the Gunn-Kinzer curve. Data taken in Colorado were significantly higher than those taken near the sea level. In fact, the ratios between the two were similar to the theoretical ratios expected from the altitude change. Data in Sumatra also showed this tendency.

Table 2: Mean drop axis ratios in rain and the standard deviations from various locations, compared with the BC-87 model and the artificial rain data

Location → D, mm↓	Beard&Chuang mean	80 m bridge data in artificial rain	Colorado	Koganei, Tokyo	Okinawa shallow rain	Okinawa Baiu-rain (normal)	Okinawa Baiu-rain (heavy) 8-9 Jun 2004	San Juan (Puerto Rico)	Sumatra, Indonesia (systematic offset of -0.03)
1.75 ± 0.25	0.943	0.963±0.042	0.944±0.034	0.942±0.036	0.948±0.035	0.951±0.040	0.948±0.039	0.946±0.036	0.949±0.037
2.25 ± 0.25	0.911	0.920±0.033	0.918±0.032	0.916±0.039	0.917±0.033	0.921±0.036	0.920±0.040	0.918±0.038	0.922±0.034
2.75 ± 0.25	0.875	0.885±0.036	0.889±0.032	0.886±0.046	0.887±0.027	0.891±0.038	0.895±0.047	0.889±0.044	0.890±0.037
3.25 ± 0.25	0.837	0.848±0.042	0.859±0.035	0.847±0.051	0.849±0.034	0.854±0.049	0.862±0.061	0.861±0.057	0.852±0.047
3.75 ± 0.25	0.798	0.810±0.055	0.834±0.007	0.809±0.061		0.818±0.069	0.830±0.080	0.840±0.079	0.813±0.063
4.25 ± 0.25	0.760	0.773±0.077		0.774±0.084		0.787±0.079	0.789±0.098	0.814±0.091	0.795±0.082
4.75 ± 0.25	0.724	0.738±0.085		0.732±0.008		0.757±0.087	0.738±0.081		
5.25 ± 0.25	0.689	0.706±0.081				0.721±0.059			
5.75 ± 0.25	0.656	0.674±0.075							
6.25 ± 0.25	0.625	0.648±0.075							
6.75 ± 0.25	0.596	0.619±0.074							
7.25 ± 0.25	0.567	0.590±0.077							
7.75 ± 0.25	0.540	0.556±0.070							
8.25 ± 0.25	0.511	0.522±0.071							
8.75 ± 0.25	0.481	0.475±0.066							

Table 3: Mean fall velocities in rain and the standard deviations from various locations, compared with the GK data and the artificial rain data

Location → D, mm↓	Gunn-Kinzer mean	Bridge experimental data (0.5 km a.s.l)	Colorado (1.5 km a.s.l)	Koganei, Tokyo	Okinawa shallow rain	Okinawa Baiu-rain (normal)	Okinawa Baiu-rain (heavy) 8-9 Jun 2004	San Juan (Puerto Rico)	Sumatra, Indonesia (0.9 km a.s.l)
1.5 ± 0.1	5.46	5.61 ± 0.25	5.70 ± 0.17	5.29 ± 0.41	*Similar*	5.35 ± 0.24	5.36 ± 0.20	5.39 ± 0.23	5.46 ± 0.24
2.0 ± 0.1	6.55	6.56 ± 0.24	6.85 ± 0.16	6.41 ± 0.45	*to*	6.61 ± 0.25	6.56 ± 0.33	6.58 ± 0.23	6.79 ± 0.25
2.5 ± 0.1	7.35	7.38 ± 0.25	7.78 ± 0.16	7.23 ± 0.41	*Okinawa*	7.49 ± 0.24	7.39 ± 0.37	7.37 ± 0.26	7.73 ± 0.25
3.0 ± 0.1	7.95	7.95 ± 0.21		7.80 ± 0.32	*Baiu*	8.10 ± 0.24	7.92 ± 0.43	7.91 ± 0.30	8.39 ± 0.26
3.5 ± 0.1	8.39	8.41 ± 0.21		8.22 ± 0.26	*normal*	8.47 ± 0.28	8.27 ± 0.45	8.28 ± 0.29	8.89 ± 0.29
4.0 ± 0.1	8.72	8.68 ± 0.20			*rain*	8.69 ± 0.32	8.50 ± 0.47	8.56 ± 0.32	9.24 ± 0.28
4.5 ± 0.1	8.96	8.87 ± 0.23						8.76 ± 0.26	
5.0 ± 0.1	9.14	8.99 ± 0.22							
5.5 ± 0.1	9.27	9.10 ± 0.21							
6.0 ± 0.1	9.37	9.13 ± 0.22							
6.5 ± 0.1	9.44	9.19 ± 0.23							
7.0 ± 0.1	9.50	9.22 ± 0.24							
7.5 ± 0.1	9.54	9.18 ± 0.22							
8.0 ± 0.1	9.57	9.10 ± 0.20							
8.5 ± 0.1	9.59	8.99 ± 0.25							

The data reported here demonstrate the capability of the 2D-VD instrument for studying the characteristics of the rain microstructure which can be put to use for a variety of applications in Radar Meteorology.

ACKNOWLEDGEMENTS

The work was sponsored by the US National Science Foundation via grant ATM-0140350. We would also like to thank Dr. G.J.Huang for assistance with the *dsd* analysis from the 2D-VD measurements and to Hiroshi Hanado for making available the 2D-VD data in Tokyo, Japan.

REFERENCES

Awaka, J., Y. Furuhama, M. Hoshiyama, and A. Nishitsuji, 1985: Model calculations of scattering properties of spherical bright-band particles made of composite dielectrics, *J. Radio Research Lab.*, **32**(136), 73-87.

Beard, K.V. and C. Chuang, 1987: A New Model for the Equilibrium Shape of Raindrops. J. Atmos. Sci., 44, 1509-1524.

Beard, K.V. and R.J. Kubesh 1991: Laboratory Measurements of Small Raindrop Distortion. Part 2: Oscillation Frequencies and Modes, *J. Atmos. Sci.*, **48**, 2245-2264.

Beard, K. V. and H. R. Pruppacher, 1969: A Determination of the Terminal Velocity and Drag of Small Water Drops by means of a Wind Tunnel. *J. Atmos. Sci.*, **26**, 1066-1072.

Brandes, E.A., G. Zhang and J. Vivekanandan, 2002: Experiments in Rainfall Estimation with a Polarimetric Radar in a Subtropical Environment. *J. Appl. Meteorol.*, **41**, 674-684.

Bringi, V.N., M. Thurai, R. Hanessen, and F. Gekat, 2005a: Dual Polarization Weather Radar Handbook 1st Ed., AMS – Gematronik GmbH, Neuss, Germany.

Bringi, V.N., M. Thurai, K. Nakagawa, G.J. Huang, T. Kobayashi, A. Adachi, H. Hanado, and S. Sekizawa, 2005b: Rainfall estimation from C-band polarimetric radar in Okinawa, Japan: Comparisons with 2D-video disdrometer and 400 MHz Wind Profiler**,** 32nd Conf. on Radar Meteorol., *this issue*, paper 11R.1, 24-29 Oct, 2005, Albuquerque, NM.

Foote, G.B. and P.S. du Toit, 1969: Terminal Velocity of Raindrops Aloft. *J. Appl. Meteorol.*, **8**, 245-253.

Goddard, J.W.F. and S.M. Cherry, 1984: The Ability of Dual-Polarisation Radar (co-polar linear) to Predict Rainfall Rate and Microwave Attenuation. *Radio Sci*., **19**, No. 1, 201-208.

Gunn, R. and G.D. Kinzer, 1949: The Terminal Velocity of Fall for Water Droplets in Stagnant Air. *J. Meteor.*, **6**, 243-248.

Kobayashi, T. and A. Adachi, 2005: Retrieval of Arbitrarily Shaped Raindrop Size Distributions from Wind Profiler Measurements. J Atmos and Ocean Tech, vol. 22, 433–442.

Randeu, W.L., M. Schönhuber and G. Lammer, 2002: Real-time Measurements and Analyses of Precipitation Micro-structure and Dynamics. *Proc. of ERAD(2002)*, 78-83.

Steiner, M., A. Waldvogel, J.W.F. Goddard, A.J. Illingworth and I.J. Caylor, 1991: A relation between mean Doppler velocity, radar reflectivity factor and differential reflectivity, IPreprints 25th Int. Conf. Radar Meteor. T, 24-28 June, Paris, AMS, 662-665.

Thurai, M. and V.N. Bringi, 2005: Drop Axis Ratios from 2D Video Disdrometer, J Atmos Ocean Tech, vol. 22, 963–975.